

A ADDITIONAL RESULTS

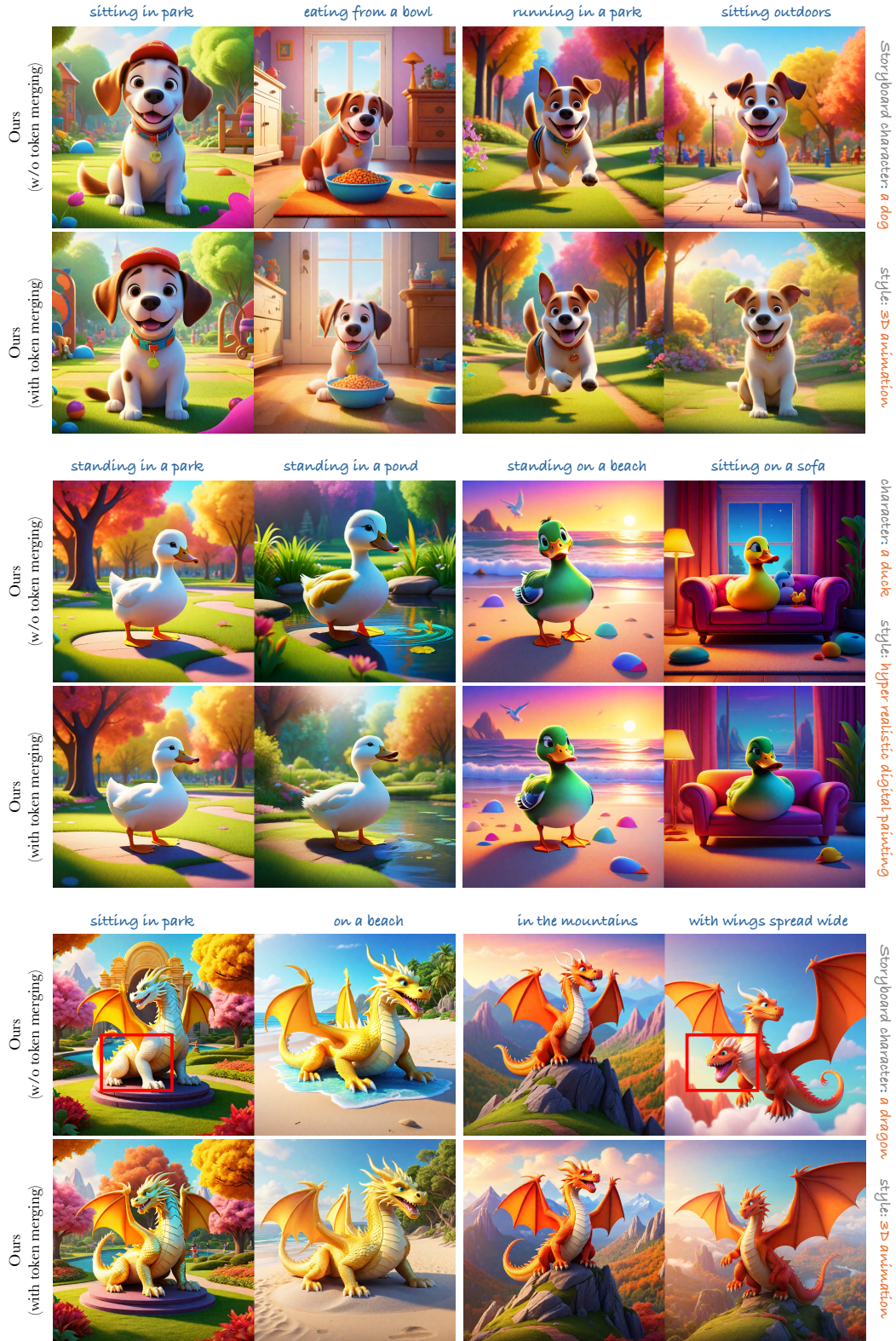


Figure 10: Additional results with and without token merging for aligning fine-grain features.



Figure 11: **Additional Results for  $N > 2$  characters.**

## B IMPLEMENTATION DETAILS

In this section, we provide further details for the implementation of our approach as well as other baselines (Ruiz et al., 2022; Zhou et al., 2024) used while reporting results in the main paper (Sec. 5).

**Model Details.** Similar to (Zhou et al., 2024; Tewel et al., 2024), we use the official SDXL model Podell et al. (2023) as the underlying pretrained text-to-image generation model while reporting results with all methods (Zhou et al., 2024; Ruiz et al., 2022; Gal et al., 2022; Ye et al., 2023) (including *storybooth* as proposed in the main paper). Results with BLIP-Diffusion (Li et al., 2024a) and Storygen (Liu et al., 2024) are reported directly using pretrained models obtained from paper-

810 authors. Similar to (Tewel et al., 2024), Dreambooth (Ruiz et al., 2022) training is done using  
 811 low-rank (LoRA) finetuning (Hu et al., 2021) with rank of 4.

812 All results are reported at  $1024 \times 1024$  resolution while using 50 inference steps during the reverse  
 813 diffusion process. Unless otherwise specified, a fixed classifier-free guidance scale (Ho & Salimans,  
 814 2022)  $\alpha_{cfg} = 5.0$  is used for all experiments. A LLaMA3-8B model AI@Meta (2024) is used as the  
 815 underlying large language model for generating storyboard layouts from the storyboard prompt  $\mathcal{P}$ .

816 **Region-Based Storyboard Generation.** A key idea behind our approach is to use region-based  
 817 planning and generation Yang et al. (2024a) in order to *a priori* localize the placement of different  
 818 characters across the storyboard. This helps us accurately apply cross-frame self-attention bounding  
 819 (refer Sec. 4) in order to allow tokens for each subject to pay attention to *only* tokens from the same  
 820 subject. However, this requires the generated images to align with the initially predicted character  
 821 layouts across the storyboard. While several region-based solutions for the same are feasible (Dahary  
 822 et al., 2024; Li et al., 2023), for simplicity we use the region-based cross-attention masking from  
 823 (Yang et al., 2024a) for ensuring adherence to the input prompt. Equal distribution of weights (Yang  
 824 et al., 2024a) are used for all character level  $\tau_i^k$  and overall-frame level storyboard prompts  $\mathcal{T}_i$ .

825 **Bounded Cross-frame Self-Attention.** We apply bounded self-attention (refer Sec. 4) both within  
 826 the same frame as well as across different frames in order to reduce inter-character leakage. The  
 827 self-attention bounding is applied predominantly on the *up-blocks* of the SDXL UNet (Podell et al.,  
 828 2023) and is used between timesteps  $t \in [1000, 200]$ . More importantly, we observe that the naive  
 829 use of self-attention bounding alone can reduce output image quality. We therefore utilize a dropout  
 830  $\beta_d = 0.5$  which allows reduces intercharacter leakage while still preserving output image quality.

831 **Token Merging.** In order to better align the fine-grain features of different subjects we use token  
 832 merging (refer Sec. 4.3) in order to place a hard-constraint on the appearance of the character features  
 833 across different frames. We use a positive  $\alpha = 0.4$  for token merging from timesteps  $t \in [950, 600]$ .  
 834 Furthermore, we also use *early negative token unmerging* (refer Sec. 4.4) with  $\alpha = -0.5$  from  
 835 timesteps  $t \in [1000, 950]$  in order to encourage pose-variance (refer Fig. 6).

## 837 C EVALUATION AND USER STUDY

838 **Datasets.** Given the training-free nature of our proposed approach, we do not rely on the use of any  
 839 public datasets. For evaluation purposes, we utilize the storyboard-prompt dataset from (Tewel et al.,  
 840 2024) which consists of 100 storyboard generation prompts with a single main subject across diverse  
 841 settings. For multi-subject evaluation, we construct an analogues multi-subject prompt dataset using  
 842 LLaMA3-8B (AI@Meta, 2024), where given a set of potential subjects (*e.g.*, *cat, dog, hedgehog,*  
 843 *owl, bear, duck etc.*) and the possible scene locations (*e.g.*, *mountains, park, beach etc.*), we prompt  
 844 the language model  $\mathcal{M}$  to generate a dataset of storyboard prompts  $\mathcal{D} = \{\mathcal{P}_1, \mathcal{P}_2, \dots, \mathcal{P}_M\}$ , (where  
 845  $M = 100$ ) placing two randomly selected subjects in different settings.

846 **Evaluation Metrics.** We also evaluate the performance of the proposed approach quantitatively, by  
 847 evaluating the text-to-image alignment and output character consistency across different storyboard  
 848 frames (refer Sec. 5 of main paper). In particular, we use the recently proposed VQAScore (Lin  
 849 et al., 2024) for evaluating text-to-image alignment, as it has been observed to show significantly  
 850 higher-correlation with the human preferences over traditionally used CLIP-Score (Hessel et al.,  
 851 2021) especially when scaling to multiple characters (Lin et al., 2024). Also, similar to Tewel et al.  
 852 (2024), Dreamsim (Fu et al., 2023) cosine similarity is used for evaluating character consistency, as  
 853 it is observed to show higher correlation with human-evaluation for image-to-image similarity as  
 854 opposed to traditionally used CLIP-I (Radford et al., 2021) and DINO (Oquab et al., 2023) scores.

855 **Human-user Study.** In addition to quantitative evaluation (refer Table 1), we also perform an  
 856 anonymous human user study wherein the T2I alignment (Lin et al., 2024) and character-consistency  
 857 (Fu et al., 2023) are evaluated by actual human users (refer Tab. 2 for results). In particular, given a  
 858 storyboard prompt  $\mathcal{P}$  and image-level prompts  $\{\mathcal{T}_1, \mathcal{T}_2, \dots, \mathcal{T}_N\}$ , the participants are shown a pair of  
 859 storyboard outputs comparing our method with prior works. The user study consists of two separate  
 860 tasks 1) Evaluating T2I Alignment and 2) Evaluating character consistency.

861 For evaluating text-to-image alignment, the participants are shown a pair of output images and the  
 862 input prompt, and asked to select the image with the best alignment between the output image and  
 863

864 input text prompt. Similarly for evaluating character-consistency, given a set of desired storyboard  
865 characters, the participants are shown a pair of storyboard outputs and asked to select the one with  
866 the better consistency for all storyboard characters. Empirically we found that unlike single-character  
867 consistency, judging cross-frame consistency for multiple characters is significantly harder even for  
868 human annotators when using  $N > 2$  frames. We therefore use  $N = 2$  frames when evaluating multi-  
869 subject consistency using human evaluation in order to get better quality annotations. Additionally,  
870 in order to remove data noise, we use a repeated comparison (control seed) for each user. Responses  
871 of users who answer differently to this repeated seed are discarded while reporting the final results.  
872 Please refer Fig. 18 for a screenshot of the quantitative human user-study setup for both tasks.  
873

## 874 D DISCUSSION AND LIMITATIONS

875

876 While the proposed approach helps improve both text-to-image alignment as well as character-  
877 consistency when scaling to multiple characters, it still has some limitations. *First*, the proposed  
878 cross-frame self-attention bounding approach relies on the use of cross-attention masking drive  
879 region-based generation Yang et al. (2024a). Thus, weaknesses of underlying region-based generation  
880 approach can sometimes become our weaknesses. Recall that region-based storyboard generation  
881 helps *a priori* localize the placements of different characters and is used for reducing inter-character  
882 leakage (refer Sec. 4). While the use of self-attention bounding further helps improve the layout  
883 consistency in the storyboard frames (refer Fig. 3 from main paper), it may still struggle in scenarios  
884 where the underlying cross-attention driven region-based generation shows poor performance. In  
885 future, the use of more advanced or off-the-shelf pretrained region-based generation models (Li et al.,  
886 2023; Dahary et al., 2024) can help consistency with the predicted storyboard layouts.

887 *Second*, we note that while negative token unmerging helps increase pose-variance, the output results  
888 may sometimes exhibit similar poses in the lack of defining action phrases in the input prompt (*e.g.*  
889 running, sitting, standing *etc.*). Nevertheless, we note that explicitly prompting the large-language  
890 model  $\mathcal{M}$  to describe the character activity in each frame can help alleviate this problem.

891 *Finally*, as noted in Tab. 1 of the main paper, while the proposed approach helps achieve better T2I  
892 alignment and character-consistency over prior works, the prompt-alignment performance decreases  
893 when scaling to multiple characters. In particular, we observe a decline in T2I alignment score for our  
894 approach from 0.78 to 0.63 when scaling to multiple characters (prior training-free *state-of-the-art*  
895 *storydiffusion* Zhou et al. (2024) declines to 0.407). This, leaves much room for improvement of  
896 consistent multi-character storyboard generation and storytelling. Combining the proposed training-  
897 free approach (Sec. 4) with selective fine-tuning the cross-frame self-attention (Guo et al., 2024)  
898 using multi-character data presents as interesting direction for future work. However, the same is out  
899 of scope of this paper, and we leave it here as direction for future research.  
900  
901  
902  
903  
904  
905  
906  
907  
908  
909  
910  
911  
912  
913  
914  
915  
916  
917



Figure 12: Additional Comparisons: comparing our approach with prior works (refer Sec. 5)

972  
973  
974  
975  
976  
977  
978  
979  
980  
981  
982  
983  
984  
985  
986  
987  
988  
989  
990  
991  
992  
993  
994  
995  
996  
997  
998  
999  
1000  
1001  
1002  
1003  
1004  
1005  
1006  
1007  
1008  
1009  
1010  
1011  
1012  
1013  
1014  
1015  
1016  
1017  
1018  
1019  
1020  
1021  
1022  
1023  
1024  
1025

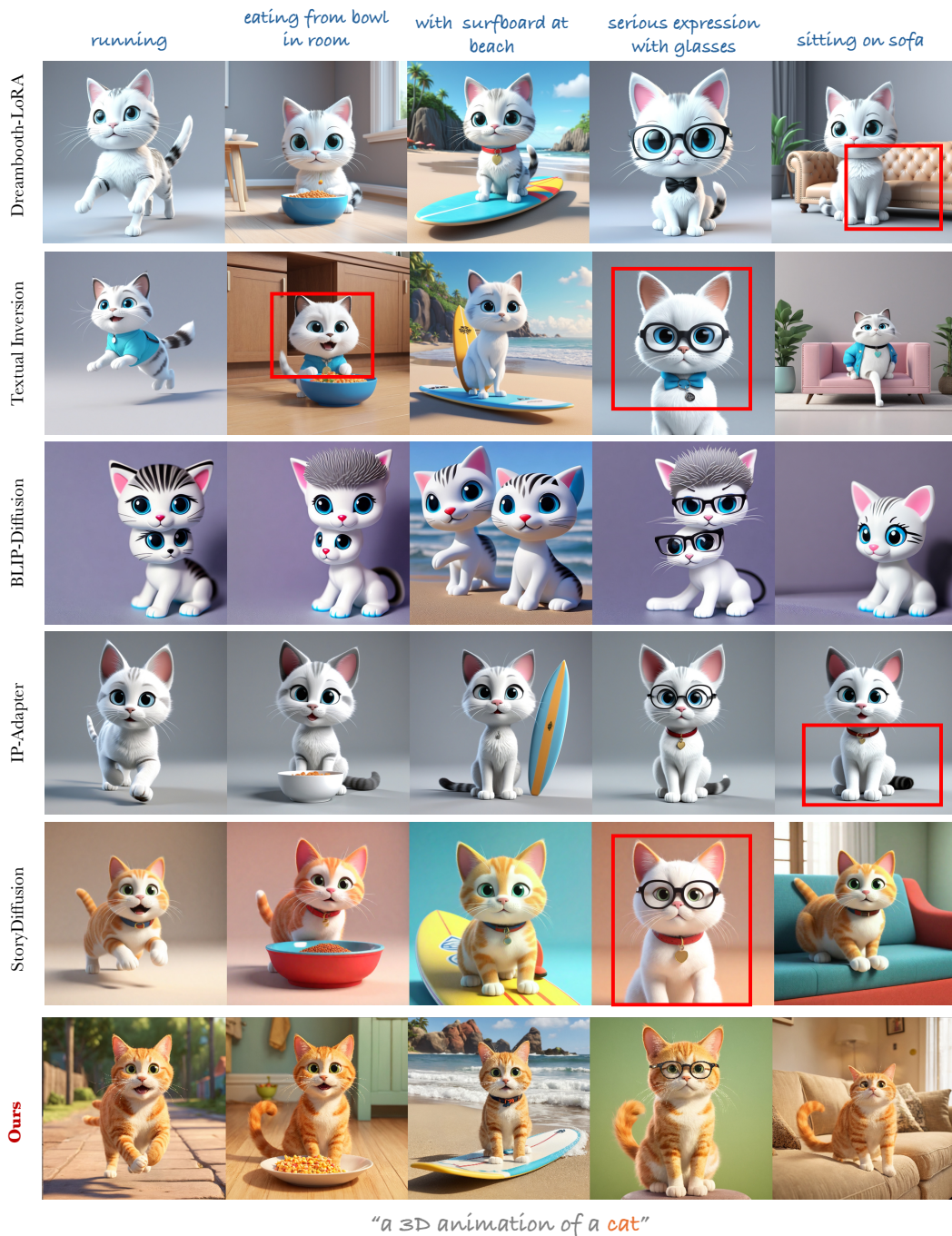


Figure 13: *Additional Comparisons*: comparing our approach with prior works (refer Sec. 5)

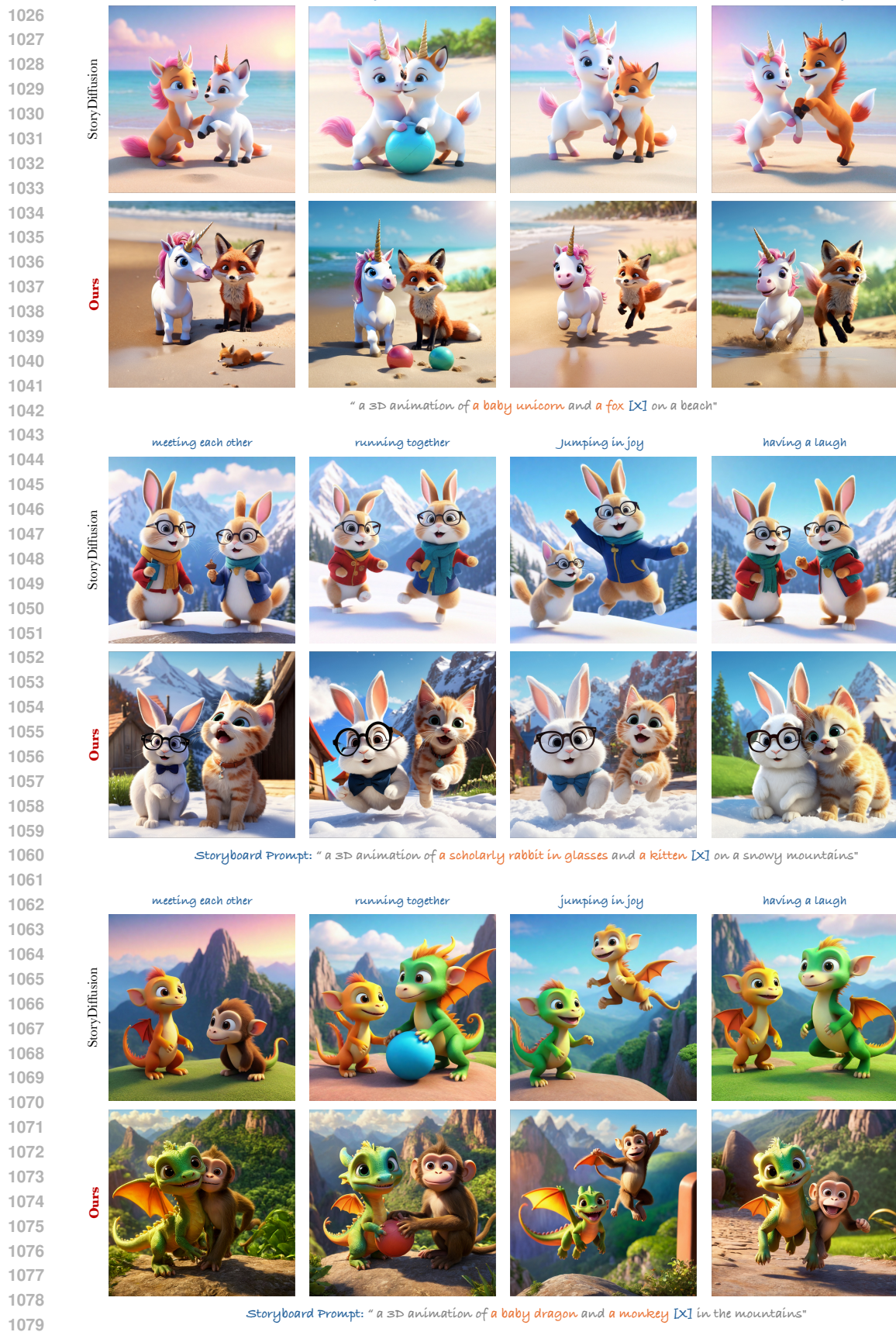


Figure 14: Additional results for multi-character storyboard generation.

1080  
 1081  
 1082  
 1083  
 1084  
 1085  
 1086  
 1087  
 1088  
 1089  
 1090  
 1091  
 1092  
 1093  
 1094  
 1095  
 1096  
 1097  
 1098  
 1099  
 1100  
 1101  
 1102  
 1103  
 1104  
 1105  
 1106  
 1107  
 1108  
 1109  
 1110  
 1111  
 1112  
 1113  
 1114  
 1115  
 1116  
 1117  
 1118  
 1119  
 1120  
 1121  
 1122  
 1123  
 1124  
 1125  
 1126  
 1127  
 1128  
 1129  
 1130  
 1131  
 1132  
 1133

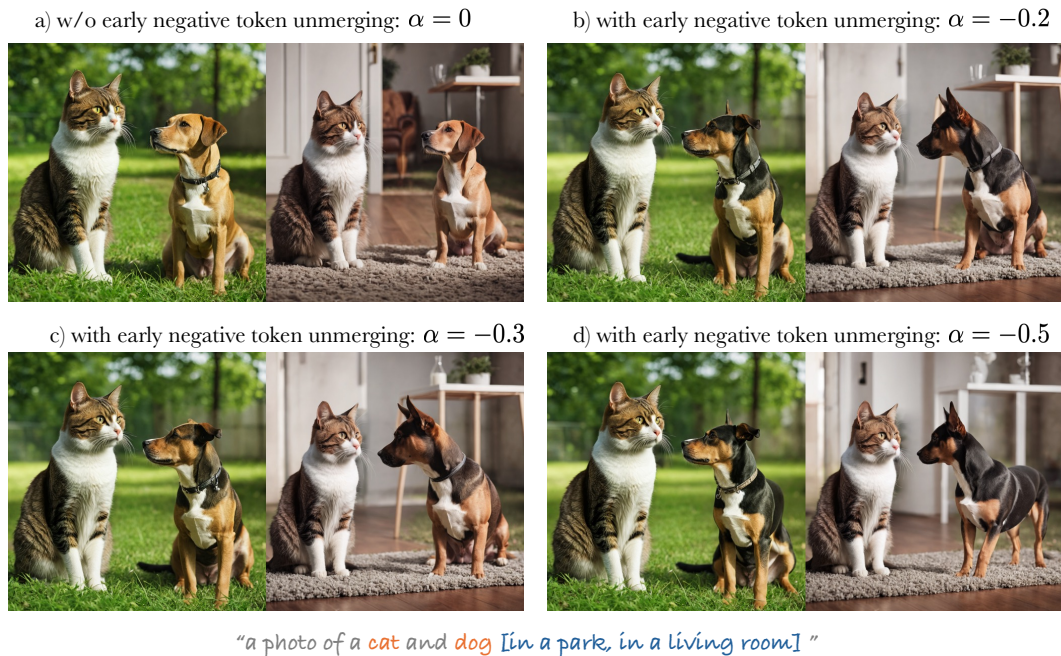


Figure 15: *Visualizing pose-variation with negative-token merging coefficient.* In order to visualize the effect of  $\alpha < 0$  for early negative token merging we generate a storyboard with a *cat and dog* in discrete settings (*park, living room*) without specifying the action (*e.g., sitting, standing etc.*). We then increase the negative-token merging coefficient  $\alpha < 0$ . We observe that without negative token unmerging the pose of both cat and dog is very similar. As the value of  $\alpha$  is gradually varied the pose variance between the subjects increase with the *dog* appearing to gradually turn to a standing position, while still maintaining consistency for both storyboard characters (*cat and dog*).



1134  
 1135  
 1136  
 1137  
 1138  
 1139  
 1140  
 1141  
 1142  
 1143  
 1144  
 1145  
 1146  
 1147  
 1148  
 1149  
 1150  
 1151  
 1152  
 1153  
 1154  
 1155  
 1156  
 1157  
 1158  
 1159  
 1160  
 1161  
 1162  
 1163  
 1164  
 1165  
 1166  
 1167  
 1168  
 1169  
 1170  
 1171  
 1172  
 1173  
 1174  
 1175  
 1176  
 1177  
 1178  
 1179  
 1180  
 1181  
 1182  
 1183  
 1184  
 1185  
 1186  
 1187



Figure 16: *Role of dropout in preserving image quality after self-attention bounding.* We observe that bounded cross-attention (BCA) computation (Yang et al., 2024a) itself can often be insufficient for removing inter-character leakage within the same frame. The *bounded self-attention* (BSA) as proposed in the paper (Sec. 4) can help reduce inter-character leakage but its naive application can result in reduction of image quality (Col-3). Therefore, despite its simplicity dropout pays a critical role in the proposed *bounded self-attention* (BSA) approach, and helps maintain output image quality while still reducing inter-character leakage. **Note:** Please note that *bounded self-attention* (BSA) as proposed in the paper (Sec. 4) also helps cross-frame inter-character leakage, however, reduction in cross-frame leakage is often not feasible unless inter-character leakage within the same frame is minimized first. Thus, the proposed approach helps address both problems in a joint formulation.

1188  
 1189  
 1190  
 1191  
 1192  
 1193  
 1194  
 1195  
 1196  
 1197  
 1198  
 1199  
 1200  
 1201  
 1202  
 1203  
 1204  
 1205  
 1206  
 1207  
 1208  
 1209  
 1210  
 1211  
 1212  
 1213  
 1214  
 1215  
 1216  
 1217  
 1218  
 1219  
 1220  
 1221  
 1222  
 1223  
 1224  
 1225  
 1226  
 1227  
 1228  
 1229  
 1230  
 1231  
 1232  
 1233  
 1234  
 1235  
 1236  
 1237  
 1238  
 1239  
 1240  
 1241

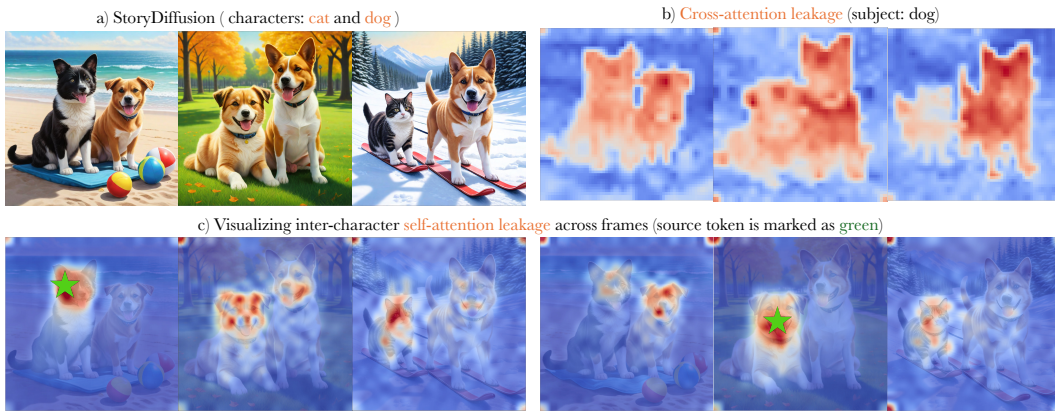


Figure 17: *Visualizing cross-frame self-attention leakage.* We observe that sharing self-attention across different frames (Zhou et al., 2024) exacerbates inter-character leakage with tokens of one subject (*dog*) paying attention to tokens of the other subject (*cat*) and *vice-versa*, across different frames. Moreover, addressing this leakage using cross-attention masking (Tewel et al., 2024) is also not feasible due to the correspondingly increased cross-attention leakage (b) between output characters.

1242  
1243  
1244  
1245  
1246  
1247  
1248  
1249  
1250  
1251  
1252  
1253  
1254  
1255  
1256  
1257  
1258  
1259  
1260  
1261  
1262  
1263  
1264  
1265  
1266  
1267  
1268  
1269  
1270  
1271  
1272  
1273  
1274  
1275  
1276  
1277  
1278  
1279  
1280  
1281  
1282  
1283  
1284  
1285  
1286  
1287  
1288  
1289  
1290  
1291  
1292  
1293  
1294  
1295

**In your opinion, which pair exhibits better consistency for both characters [cat and dog]?**

Please make your choice based on:  
 1. Check whether both characters [cat and dog] are present in each frame  
 2. Check whether the visual appearance of each character is similar across the frames

**User Response**

Which pair of images exhibits better character consistency across the output frames?

Left<sup>[1]</sup>  Tie<sup>[2]</sup>  Right<sup>[3]</sup>

Hotkey TIPS

**Hotkey tip for efficient labelling**

For more efficient labelling, the demo supports use of hotkeys (1: left, 2: tie, 3: right) for selecting different choices during data annotation. Please feel free to make use of the same if more convenient.

(a) Setup for user-study evaluating multi-character consistency (refer Sec. 5)

**In your opinion, which image is a better match for the following input prompt?**

1 | a hyper-realistic digital painting a hedgehog and a cat sitting in a park

**User Response**

In your opinion, which image is a better match for the following input prompt?

Left<sup>[1]</sup>  Tie<sup>[2]</sup>  Right<sup>[3]</sup>

(b) Setup for user-study evaluating multi-character consistency (refer Sec. 5).

Figure 18: Setup for user-study comparing our method with prior works (refer Sec. 5)

## REFERENCES

- 540  
541  
542 AI@Meta. Llama 3 model card. 2024. URL [https://github.com/meta-llama/llama3/](https://github.com/meta-llama/llama3/blob/main/MODEL_CARD.md)  
543 [blob/main/MODEL\\_CARD.md](https://github.com/meta-llama/llama3/blob/main/MODEL_CARD.md). 16
- 544 Omri Avrahami, Amir Hertz, Yael Vinker, Moab Arar, Shlomi Fruchter, Ohad Fried, Daniel Cohen-Or,  
545 and Dani Lischinski. The chosen one: Consistent characters in text-to-image diffusion models. In  
546 *ACM SIGGRAPH 2024 Conference Papers*, pp. 1–12, 2024. 1, 3
- 547 Daniel Bolya, Cheng-Yang Fu, Xiaoliang Dai, Peizhao Zhang, Christoph Feichtenhofer, and Judy  
548 Hoffman. Token merging: Your vit but faster. *arXiv preprint arXiv:2210.09461*, 2022. 3
- 550 Omer Dahary, Or Patashnik, Kfir Aberman, and Daniel Cohen-Or. Be yourself: Bounded attention  
551 for multi-subject text-to-image generation. *arXiv preprint arXiv:2403.16990*, 2024. 1, 5, 16, 17
- 552 Weixi Feng, Wanrong Zhu, Tsu-jui Fu, Varun Jampani, Arjun Akula, Xuehai He, Sugato Basu,  
553 Xin Eric Wang, and William Yang Wang. Layoutgpt: Compositional visual planning and generation  
554 with large language models. *Advances in Neural Information Processing Systems*, 36, 2024. 3
- 555 Zhangyin Feng, Yuchen Ren, Xinmiao Yu, Xiaocheng Feng, Duyu Tang, Shuming Shi, and Bing Qin.  
556 Improved visual story generation with adaptive context modeling. *arXiv preprint arXiv:2305.16811*,  
557 2023. 1, 3
- 559 Stephanie Fu, Netanel Tamir, Shobhita Sundaram, Lucy Chai, Richard Zhang, Tali Dekel, and Phillip  
560 Isola. Dreamsim: Learning new dimensions of human visual similarity using synthetic data. *arXiv*  
561 *preprint arXiv:2306.09344*, 2023. 9, 16
- 562 Rinon Gal, Yuval Alaluf, Yuval Atzmon, Or Patashnik, Amit H Bermano, Gal Chechik, and Daniel  
563 Cohen-Or. An image is worth one word: Personalizing text-to-image generation using textual  
564 inversion. *arXiv preprint arXiv:2208.01618*, 2022. 1, 3, 7, 9, 10, 15
- 566 Yuwei Guo, Ceyuan Yang, Anyi Rao, Zhengyang Liang, Yaohui Wang, Yu Qiao, Maneesh Agrawala,  
567 Dahua Lin, and Bo Dai. Animatediff: Animate your personalized text-to-image diffusion models  
568 without specific tuning. *International Conference on Learning Representations*, 2024. 17
- 569 Jack Hessel, Ari Holtzman, Maxwell Forbes, Ronan Le Bras, and Yejin Choi. Clipscore: A reference-  
570 free evaluation metric for image captioning. *arXiv preprint arXiv:2104.08718*, 2021. 16
- 572 Jonathan Ho and Tim Salimans. Classifier-free diffusion guidance. *arXiv preprint arXiv:2207.12598*,  
573 2022. 16
- 574 Edward J Hu, Yelong Shen, Phillip Wallis, Zeyuan Allen-Zhu, Yanzhi Li, Shean Wang, Lu Wang,  
575 and Weizhu Chen. Lora: Low-rank adaptation of large language models. *arXiv preprint*  
576 *arXiv:2106.09685*, 2021. 16
- 578 Hyeonho Jeong, Gihyun Kwon, and Jong Chul Ye. Zero-shot generation of coherent storybook from  
579 plain text story using diffusion models. *arXiv preprint arXiv:2302.03900*, 2023. 1, 3
- 580 Dongxu Li, Junnan Li, and Steven Hoi. Blip-diffusion: Pre-trained subject representation for  
581 controllable text-to-image generation and editing. *Advances in Neural Information Processing*  
582 *Systems*, 36, 2024a. 1, 3, 7, 9, 10, 15
- 584 Xirui Li, Chao Ma, Xiaokang Yang, and Ming-Hsuan Yang. Vidtoime: Video token merging for  
585 zero-shot video editing. In *Proceedings of the IEEE/CVF Conference on Computer Vision and*  
586 *Pattern Recognition*, pp. 7486–7495, 2024b. 3, 7
- 587 Yuheng Li, Haotian Liu, Qingyang Wu, Fangzhou Mu, Jianwei Yang, Jianfeng Gao, Chunyuan Li,  
588 and Yong Jae Lee. Gligen: Open-set grounded text-to-image generation. In *Proceedings of the*  
589 *IEEE/CVF Conference on Computer Vision and Pattern Recognition*, pp. 22511–22521, 2023. 3,  
590 16, 17
- 591 Zhiqiu Lin, Deepak Pathak, Baiqi Li, Jiayao Li, Xide Xia, Graham Neubig, Pengchuan Zhang, and  
592 Deva Ramanan. Evaluating text-to-visual generation with image-to-text generation. *arXiv preprint*  
593 *arXiv:2404.01291*, 2024. 9, 16

- 594 Chang Liu, Haoning Wu, Yujie Zhong, Xiaoyun Zhang, Yanfeng Wang, and Weidi Xie. Intelligent  
595 grimm-open-ended visual storytelling via latent diffusion models. In *Proceedings of the IEEE/CVF*  
596 *Conference on Computer Vision and Pattern Recognition*, pp. 6190–6200, 2024. [1](#), [2](#), [3](#), [7](#), [9](#), [10](#),  
597 [15](#)
- 598 Maxime Oquab, Timothée Darcet, Théo Moutakanni, Huy Vo, Marc Szafraniec, Vasil Khalidov,  
599 Pierre Fernandez, Daniel Haziza, Francisco Massa, Alaaeldin El-Nouby, et al. Dinov2: Learning  
600 robust visual features without supervision. *arXiv preprint arXiv:2304.07193*, 2023. [16](#)
- 601 William Peebles and Saining Xie. Scalable diffusion models with transformers. *arXiv preprint*  
602 *arXiv:2212.09748*, 2022. [1](#)
- 603 Dustin Podell, Zion English, Kyle Lacey, Andreas Blattmann, Tim Dockhorn, Jonas Müller, Joe  
604 Penna, and Robin Rombach. Sdxl: Improving latent diffusion models for high-resolution image  
605 synthesis. *arXiv preprint arXiv:2307.01952*, 2023. [7](#), [9](#), [15](#), [16](#)
- 606 Alec Radford, Jong Wook Kim, Chris Hallacy, Aditya Ramesh, Gabriel Goh, Sandhini Agarwal,  
607 Girish Sastry, Amanda Askell, Pamela Mishkin, Jack Clark, et al. Learning transferable visual  
608 models from natural language supervision. In *International Conference on Machine Learning*, pp.  
609 8748–8763. PMLR, 2021. [16](#)
- 610 Robin Rombach, Andreas Blattmann, Dominik Lorenz, Patrick Esser, and Björn Ommer. High-  
611 resolution image synthesis with latent diffusion models, 2021. [1](#)
- 612 Nataniel Ruiz, Yuanzhen Li, Varun Jampani, Yael Pritch, Michael Rubinstein, and Kfir Aberman.  
613 Dreambooth: Fine tuning text-to-image diffusion models for subject-driven generation. *arXiv*  
614 *preprint arXiv:2208.12242*, 2022. [1](#), [2](#), [3](#), [7](#), [9](#), [10](#), [15](#), [16](#)
- 615 Yoad Tevel, Omri Kaduri, Rinon Gal, Yoni Kasten, Lior Wolf, Gal Chechik, and Yuval Atzmon.  
616 Training-free consistent text-to-image generation. *ACM Transactions on Graphics (TOG)*, 43(4):  
617 1–18, 2024. [1](#), [2](#), [3](#), [7](#), [9](#), [15](#), [16](#), [23](#)
- 618 Khai N Truong, Gillian R Hayes, and Gregory D Abowd. Storyboarding: an empirical determination  
619 of best practices and effective guidelines. In *Proceedings of the 6th conference on Designing*  
620 *Interactive systems*, pp. 12–21, 2006. [1](#)
- 621 Yuxiang Wei, Yabo Zhang, Zhilong Ji, Jinfeng Bai, Lei Zhang, and Wangmeng Zuo. Elite: Encoding  
622 visual concepts into textual embeddings for customized text-to-image generation. *arXiv preprint*  
623 *arXiv:2302.13848*, 2023. [3](#)
- 624 Bichen Wu, Ching-Yao Chuang, Xiaoyan Wang, Yichen Jia, Kapil Krishnakumar, Tong Xiao,  
625 Feng Liang, Licheng Yu, and Peter Vajda. Fairy: Fast parallelized instruction-guided video-to-  
626 video synthesis. In *Proceedings of the IEEE/CVF Conference on Computer Vision and Pattern*  
627 *Recognition*, pp. 8261–8270, 2024. [3](#)
- 628 Ling Yang, Zhaochen Yu, Chenlin Meng, Minkai Xu, Stefano Ermon, and CUI Bin. Mastering text-  
629 to-image diffusion: Recaptioning, planning, and generating with multimodal llms. In *Forty-first*  
630 *International Conference on Machine Learning*, 2024a. [2](#), [3](#), [4](#), [5](#), [16](#), [17](#), [22](#)
- 631 Shuai Yang, Yuying Ge, Yang Li, Yukang Chen, Yixiao Ge, Ying Shan, and Yingcong Chen.  
632 Seed-story: Multimodal long story generation with large language model. *arXiv preprint*  
633 *arXiv:2407.08683*, 2024b. [1](#), [2](#), [3](#), [7](#), [9](#)
- 634 Hu Ye, Jun Zhang, Sibio Liu, Xiao Han, and Wei Yang. Ip-adapter: Text compatible image prompt  
635 adapter for text-to-image diffusion models. *arXiv preprint arXiv:2308.06721*, 2023. [1](#), [7](#), [8](#), [9](#), [10](#),  
636 [15](#)
- 637 Zhengqing Yuan, Ruoxi Chen, Zhaoxu Li, Haolong Jia, Lifang He, Chi Wang, and Lichao Sun.  
638 Mora: Enabling generalist video generation via a multi-agent framework. *arXiv preprint*  
639 *arXiv:2403.13248*, 2024. [3](#)
- 640 Zhuosheng Zhang, Aston Zhang, Mu Li, Hai Zhao, George Karypis, and Alex Smola. Multimodal  
641 chain-of-thought reasoning in language models. *arXiv preprint arXiv:2302.00923*, 2023. [4](#)

648 Canyu Zhao, Mingyu Liu, Wen Wang, Jianlong Yuan, Hao Chen, Bo Zhang, and Chunhua Shen.  
649 Moviedreamer: Hierarchical generation for coherent long visual sequence, 2024. URL <https://arxiv.org/abs/2407.16655>. 1, 3  
650  
651  
652 Yupeng Zhou, Daquan Zhou, Ming-Ming Cheng, Jiashi Feng, and Qibin Hou. Storydiffusion: Con-  
653 sistent self-attention for long-range image and video generation. *arXiv preprint arXiv:2405.01434*,  
654 2024. 1, 2, 3, 4, 7, 9, 10, 15, 17, 23  
655  
656  
657  
658  
659  
660  
661  
662  
663  
664  
665  
666  
667  
668  
669  
670  
671  
672  
673  
674  
675  
676  
677  
678  
679  
680  
681  
682  
683  
684  
685  
686  
687  
688  
689  
690  
691  
692  
693  
694  
695  
696  
697  
698  
699  
700  
701